

Dynamic Characteristics of the Skull with the Neck Effect

B.W. Huang¹, Y.-W. Ou¹, C.H. Chang², G.S. Chen¹, K.T. Yen³, J.-G. Tseng^{4*}

¹Graduate Institute of Mechatronics Engineering, Cheng Shiu University, Kaohsiung, Taiwan, R.O.C.

²Neurosurgery department, Mackay Memorial Hospital Taitung Branch, Taitung, Taiwan, R.O.C.

³Department of Leisure and Sport Management, Cheng Shiu University, Kaohsiung, Taiwan, R.O.C.

⁴Bachelor Program of Medical Engineering, Cheng Shiu University, Kaohsiung, Taiwan, R.O.C.

Abstract: The human head is a combination of the variety of different tissues of the skull, brain, cerebellar, brainstem, cerebrospinal fluid (CSF), and neck bone, etc. The differences of both skull and neck bone combined reaction and pure skull reaction are discussed in the analysis. Finite element method (FEM) is employed not only to analyze the natural vibration modes but also to understand the reaction of the combinations of the skull and neck bone. To evaluate the realistic dynamic behavior of the human head, white light scanner and 3D graphics software are used to construct the skull and neck bone combined model. After confirming the correctness of the skull and neck bone combined model and pure skull model, respectively, the real human bone properties are brought into models and the comparisons about the simulated normal modes analysis of the two models are obtained. The found natural frequencies of the human skull-neck structure will help to avoid the injuries on head or neck.

[B.W. Huang, Y.-W. Ou, C.H. Chang, et al. **Dynamic Characteristics of the Skull with the Neck Effect.** *Life Sci J* 2013;10(2):265-270] (ISSN:1097-8135). <http://www.lifesciencesite.com>. 42

Keywords: Head, Skull, Brain, Neck Bone.

1. Introduction

Human head, including skull and neck, is one of the most important parts of human life. Whenever there are accidents caused by traffic, football, boxing, hockey and other sports, or unexpected situations in the daily life, human's head and neck injuries are the major ones due to impact with other objects or fall down.

Camacho et al. [1] proposed that when contact between the impact surface and the head will cause the injury on head and neck. To observe the principle of the kinematics and kinetics, the model includes not only the rigid vertebrae interconnected by assemblies of nonlinear springs and dashpots, but also a finite element shell model of the skull. Thali et al. [2] studied wound morphology and created a "skin-skull-brain model" to simulate the actual situation of a real ballistic missile injury by the bullet. Yoganandan et al. [3] presented a biomechanics analysis of head injury with an emphasis on the tolerance of the skull to lateral impacts. Human cadavers were not only subjected to static and various types of dynamic loading (drop, impact, etc.) experiments but also were provided relative changes in the anatomical parts of the human skull depend on different impact angle. Meyer et al. [4] put forward, experimentally and theoretically, the cervical spine behavior during impact was the most complex. Natural frequencies and mode shapes of the head-neck system were identified in three dimensions. Zong et al. [5] used the three-dimensional finite element model to evaluate the possibility of injury due to head impact load and structural intensity (SI) via experimental

biomechanics method. The head model is computed in SI field for three cases, namely frontal, rear and side impacts. Wang et al. [6] used FEM to obtain the head dynamic reaction of stress, strain, strain energy density and intracranial pressure under impact load. Head Injury Criterion (HIC) and energy absorption criteria were found to be consistent to head trauma and dynamic response in each partial skull under different position of impact loads. Gong et al. [7] used the full size mannequin in a car impact test system. For the environment simulation, the test includes the injury by seats and seat belts in a car accident or to evaluate the head intracranial pressure and neck injury caused by the actions of non-contact type of loading when the car is braking. Tu et al. [8] used a dynamic elastic-plastic finite element model to simulate a process of a Kirschner pin drilling through the bone. Chatelin et al. [9] discussed that the elongation of axons is thought to result in brain damage and to lead to Diffuse Axonal Injuries (DAI) in head trauma situation. After detailing the coupling technique between Diffusion Tensor Imaging (DTI) atlas and the head FE model, two head trauma cases presenting different DAI injury levels are reconstructed and analyzed with the developed methodology as an illustration of axonal elongation computation. The results show that the anisotropic brain structures can be realistically implemented into an existing finite element model of the brain. Li et al. [10] put forward a skull completion framework basis of symmetry and surface matching. Symmetric region on the skull, mapping template damaged skull were identified, then used transplanted area template to fill

and fix this skull model. Samir M. Badawi et al. [11] used MRI image enhancements using different contrast agents. And considered the magnetized-saline (MS) as a new MRI brain contrast agent (CA). Leading to the result; magnetized saline injection affect signal intensity and enhance contrast in MRI brain images. Bartsch et al. [12] used Anthropomorphic Test Device (ATD), mostly in automotive or military test, as the alternative in the most extensive human impact test. This ATD is found useful in the applications to evaluate the athletic helmet protectively to quantify the head impact dosage and to estimate the injury risk. Linear or angular acceleration, velocity of center of gravity of the head, occipitals-cervical mechanics and neck stiffness were all obtained to develop the impact tests standards of head and neck injuries. Huang et al. [13] examined the fundamental dynamic characteristic of both the solid and hollow femur, experimentally and numerically. And imported to the finite element package, ANSYS, to perform the analysis. Roberts et al. [14] built the finite element model of a human head to study the influence of the dynamics and kinematics of the explosion wave. More calculation in the parameter of the model with human brain that was placed in front of the shock tube and also was excited by its fluid, was obtained. Wei [15] verified the correctness of a synthesis skull model (plastic material of Low Density Polyethylene-LDPE) by experiments and FEM, substituted human parameter of skull, brain, CSF, etc., determined the actual boundary conditions, and external impact forces, and obtained dynamic internal brain displacement, natural frequencies and mode shapes from the modal analysis. Huang et al. [16] investigated the dynamic property of cranium by experimental and theoretical analysis through skull model made in polystyrene. Reverse engineering analysis is adopted to build up geometric 3D skull CAD model by transferring this 3D skull CAD model into ANSYS (FEA package) acceptable model. Kleiven et al. [17] evaluated whether the variation of human head size results in different outcome regarding intracranial responses following a direct impact and concluded that the size dependence of the intracranial stresses associated with injury was not predicted by the HIC. Tzeng et al. [18] used the impulse technique to execute modal test by impact hammer and accelerometers to get the natural frequencies and damping ratio of the dry human skull experimentally and theoretically. Chiu et al. [19] had the comparison on the natural frequencies of 3D FE models between the plain skull and the skull with brain.

The neck supports the weight of the head and protects the nerves that carry sensory and motor information from the brain down to the rest of the body. In addition, the neck is highly flexible and allows the head to turn and flex in all directions. The cervical

spine (neck) is comprised of seven vertebrae (C1 ~ C7), that begin at the base of the skull and extend down to the thoracic spine. The cervical vertebrae are composed of cylindrical bones (vertebral bodies) that lie in front of the spinal cord, and work with the muscles, joints, ligaments and tendons to provide support, structure and stabilization to the neck.

This research studies the neck effect of the human skull and neck combined structure (skull-neck) via vibration modal analysis and compares the results with pure skull structure. To understand the dynamic characteristics of the human skull-neck structure will help to avoid the injuries on head or neck.

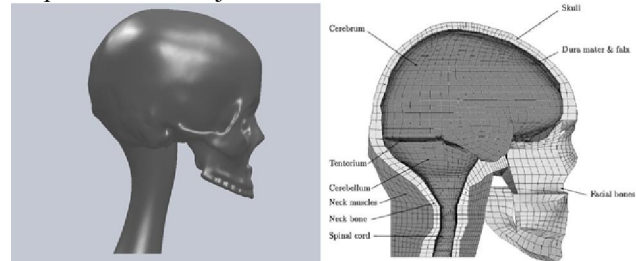


Figure 1. Size comparison between skull-neck 3D solid model (left) and Kleiven's model (right) [17]

2. Finite element analysis methods

This article is based on previous experimental and analytical study of skull and brain structure [15]. Some changes are made to improve the model. To simulate real human head situation, a simplified human cervical vertebra (neck bone) component is built to join the skull model by 3D graphical software. The size of the skull is compared with Kleiven's model [14] as shown in Figure 1. The 3D graphs of the skull-neck structure is then imported into finite element analysis software ANSYS to do the normal mode analysis. The real human bone material parameters are used for the analysis. Flow chart for finite element analysis of this research is shown in Figure 2. ANSYS 3D Solid187 element (Figure 3), suitable for irregular mesh, is selected for the skull-neck structure to reduce the poor precision problem in free mesh operation. Skull-neck and pure skull FE model [15 16] are shown in Figure 4. After generating the element mesh of skull and neck bones, the next step is to set the fixed boundary conditions at the end of the skull or at the neck bone for two different models, respectively. Finally, select the projects to get the solution of modal analysis and to post process the results of the analysis. The mesh elements convergence tests of fundamental frequency are performed for both skull-neck and pure skull models. If the convergence analysis diagram presents a divergence phenomenon, one must return to pre-treatment section, adjust the settings of material parameters, contact conditions, or boundary conditions and begin to re-analyze again.

3. Results and Discussions

The results of natural frequencies and mode shapes of the two models, pure skull model and skull-neck model, are shown, compared and discussed separately in the following subsections.

3.1 Modal analysis results of pure skull model

The fixed boundary conditions at the occipital condyle, connecting atlas (C1) of the cervical spine (neck), of the pure skull model is shown in Figure 5. The mesh element convergence test of the first natural frequency of pure skull model is obtained, as shown in Figure 6.

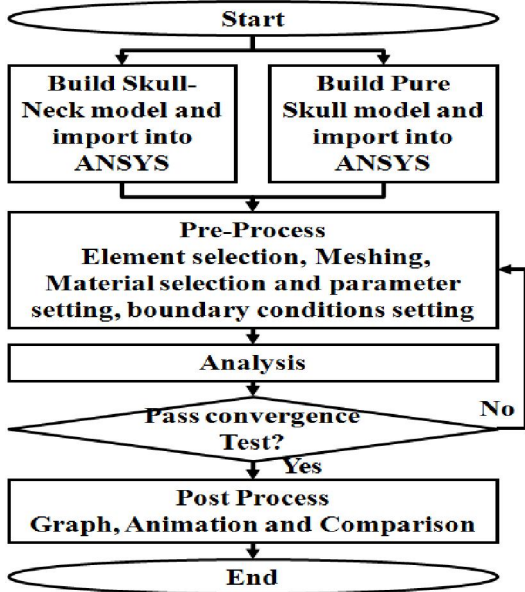


Figure 2. Flow chart of finite element analysis

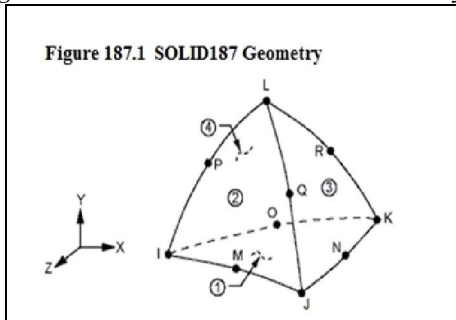


Figure 3. Geometry of ANSYS Solid187 element

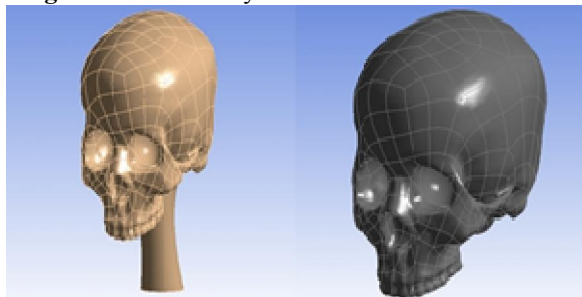


Figure 4. Skull-neck (left) and pure skull (right) [15 16] FE model

When the number of elements reaches and is over 12,000, the first natural frequency converges to 149.1 Hz. Therefore, 12,000 elements are used for the modal analysis simulation. Then, real human bone material parameters, Young's modulus, Poisson's ratio, and density are set in the FE model, as shown in Table 1.

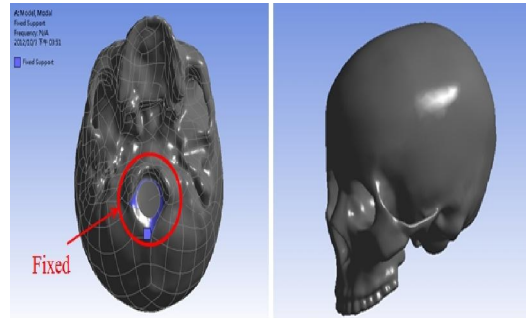


Figure 5. Fixed boundary condition at the occipital condyle of the pure skull model [15, 16]

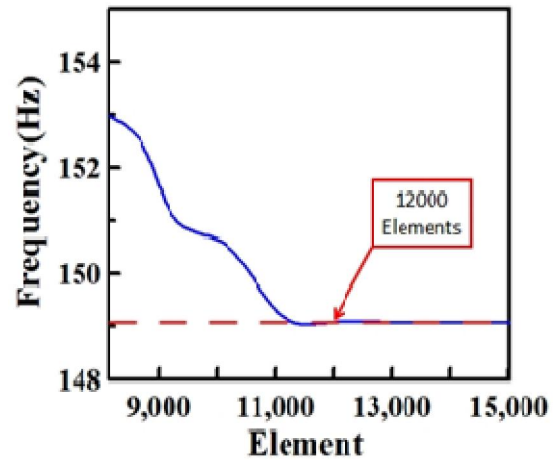


Figure 6. Pure skull model convergence analysis of the first natural frequency

Table 1. Human skull-neck and pure skull material properties table [15, 19]

Mechanical properties	values
Young's modulus	6500 MPa
Poisson Ratio	0.25
Density	2.1326 g/cm ³

Table 2. Finite element natural vibration frequency of pure skull model

Mode	Natural frequencies (Hz)
1	149.1
2	215.7
3	432.1
4	860.2

Table 2 is the list of first four natural frequencies of pure skull. The first mode shape, front-rear swing mode, with frequency 149.1Hz of the pure skull, is shown in Figure 7.

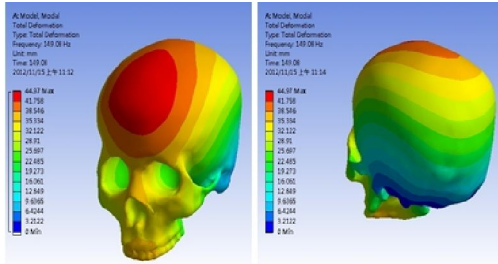


Figure 7. First mode shape of pure skull model at 149.1 Hz (front-rear swing vibration)

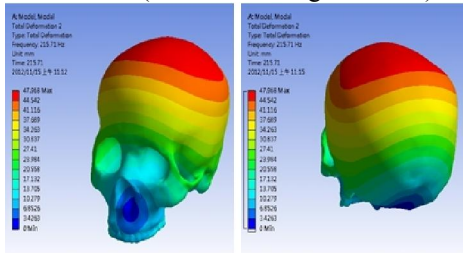


Figure 8. Second mode shape of pure skull model at 215.7 Hz (right-left swing vibration)

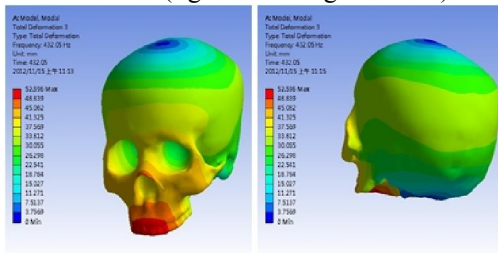


Figure 9. Third mode shape of pure skull model at 432.1 Hz (rotating swing vibration)

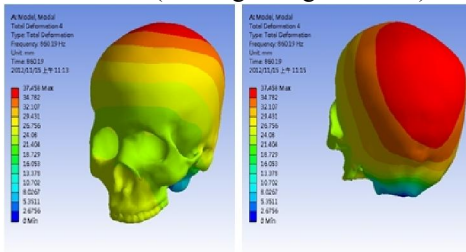


Figure 10. Fourth mode shape of pure skull model at 860.2 Hz (up-down vibration)

Maximum displacement occurs at the forehead of the skull. The 2nd mode shape, left-right swing mode, with frequency 215.7 Hz of the pure skull, is shown in Figure 8. Maximum displacement occurs at the middle top of the skull. The 3rd mode shape, rotating mode (around the axis parallel to the neck), with frequency 432.1 Hz of the pure skull, is shown in Figure 9. Maximum displacement occurs at the middle palate of the skull. The 4th mode shape, up-down stretching mode, with frequency 860.2 Hz of the pure skull, is shown in Figure 10. Maximum displacement occurs at the top of the skull and the curve surface of middle of back of the skull.

3.2 Modal analysis results of skull-neck model

The fixed boundary conditions at the end of the neck bone, the seventh cervical vertebrae (C7 or vertebra prominens), of the skull-neck model is shown in Figure 11. The mesh element convergence test of the first natural frequency of skull-neck model is obtained, as shown in Figure 12. When the number of elements reaches and is over 15,000, the first natural frequency converges to 88.7 Hz. Therefore, 15,000 elements are used for the modal analysis simulation. Similar to the pure skull model, real human bone material parameters, Young's modulus, Poisson's ratio, and density are also set in the FE model, as shown in Table 1.

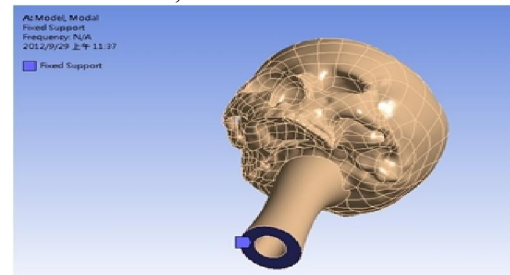


Figure 11. Fixed boundary condition of skull-neck model at C7 or vertebra prominens

Table 3 is the list of first four natural frequencies of the skull-neck structure. The first mode shape, front-rear swing mode, with frequency 88.7 Hz of the skull-neck model, is shown in Figure 13. The 2nd mode shape, left-right swing mode, with frequency 99.4 Hz of the skull-neck, is shown in Figure 14.

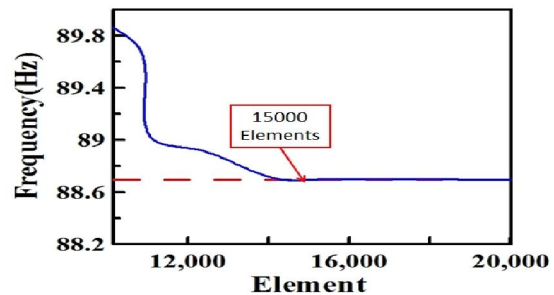


Figure 12. Skull-neck model convergence analysis of the first natural frequency

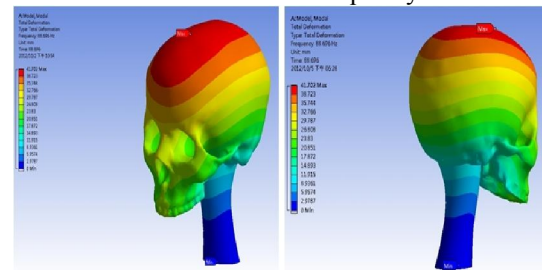


Figure 13. First mode shape of skull-neck model at 88.7 Hz (front-rear swing vibration)

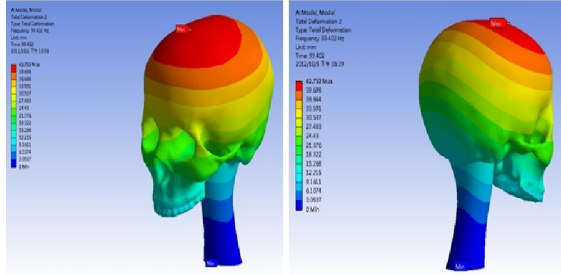


Figure 14. Second mode shape of skull-neck model at 99.4 Hz (right-left swing vibration)

Table 3. Natural frequencies of skull-neck model

Mode	Natural frequencies (Hz)
1	88.7
2	99.4
3	171.1
4	399.4

Maximum displacement occurs at the middle top of the skull. The 3rd mode shape is a rotating mode (around the axis parallel to the neck), with frequency 171.1 Hz of the skull-neck model. Maximum displacement occurs at the middle palate of the skull. The 4th mode shape is an up-down stretching mode, with frequency 399.4 Hz of the skull-neck model. Maximum displacement occurs at the top of the skull and the curve surface of middle of back of the skull.

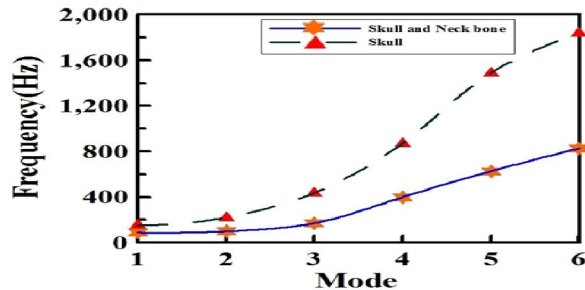


Figure 15. Natural frequencies comparison between skull-neck and pure skull models

From the results of above-mentioned analysis, both pure skull and skull-neck models are adopted the real human skull and neck bone material parameters, the boundary conditions clamped at occipital condyle and the seventh cervical vertebrae of each model, respectively, as show in Figure 5 and Figure 11. The comparison of natural frequencies between skull-neck models and pure skull are shown in Figure 15. First six modes of the skull-neck model, shown in blue solid line (star markers), are 88.7 Hz, 99.4 Hz, 171.1 Hz, 399.4 Hz, 626.7 Hz, 827.3 Hz. The first six modes of the pure skull model, shown in dark green dashed line (triangle markers), are 149.1 Hz, 215.7 Hz, 432.1 Hz, 860.2 Hz, 1488 Hz, 1839.2 Hz. It is obvious that each natural frequency of the skull-neck model is lower than the corresponding one of pure skull model.

The reason that the natural frequencies of skull-neck model are generally lower than that of pure skull model is due to the different geometry of the two models. The skull-neck system behaves like a hollow beam with added end mass. The fundamental bending and torsion modes of the hollow beam of the skull-neck system are lower than the pure skull swing and rotating modes. Hence, the skull-neck model is easier to be excited by lower frequencies to reach the resonance phenomenon than the pure skull model is. In other words, the skull-neck structure is more vulnerable than pure skull structure from vibration normal mode (resonance phenomenon) point of view.

4. Conclusion

The neck effect of the human head, with real bone material parameters, is studied via vibration modal analysis comparison between skull-neck and pure skull models. Several effects are summarized as follows:

- (1) The skull-neck system behaves like a hollow beam with added end mass. Due to the beam effect, the fundamental bending and torsion modes of the hollow beam of the skull-neck system are lower than the pure skull swing and rotating modes.
- (2) Since the skull-neck model will be excited easier by lower frequencies to reach the resonance phenomenon than the pure skull model is, skull-neck structure is more vulnerable than pure skull structure from vibration normal mode (resonance phenomenon) point of view.
- (3) Results indicate that the neck affects the dynamic characteristics of the skull-neck structure significantly.

5. References

1. D.L.A. Camacho, R.W. Nightingale, B.S. Myers, "Surface friction in near-vertex head and neck impact increases risk of injury," *Journal of Biomechanics*, Vol. 32 (3), pp. 293-301, 1999.
2. M.J. Thali, B.P. Kneubuehl, U. Zollinger, R. Dimhofer, "The Skin-skull-brain model: a new instrument for the study of gunshot effects," *Forensic Science International*, Vol. 125 (2-3), pp. 178-189, 2002.
3. N. Yoganandan, F.A. Pintar, "Biomechanics of temporo-parietal skull fracture," *Clinical Biomechanics*, Vol. 19, pp. 225-239, 2004.
4. F. Meyer, R. Willinger, F. Legall, "The importance of modal validation for biomechanical models, demonstrated by application to the cervical spine," *Finite Elements in Analysis and Design*, Vol. 40, pp. 1835-1855, 2004.
5. Z. Zong, H.P. Lee, C. Lu, "A three-dimensional human head finite element model and power flow in a human head subject to impact loading," *Journal*

- of Biomechanics, Vol. 39, pp. 284-292, 2006.
6. Fang Wang, Heow Pueh Lee, Chun Lu, "Effects of head size and morphology on dynamic responses to impact loading," *Medical & Biological Engineering & Computing*, Vol. 45, pp. 747-757, 2007.
 7. S.W. Gong, H.P. Lee, C. Lu, "Computational simulation of the human head response to non-contact impact," *Computers and Structures*, Vol. 86, pp. 758-770, 2008.
 8. Y.-K. Tu, Y.-Y. Hong, Y.-C. Chen, "Finite element modeling of kirschner pin and bone thermal contact during drilling," *Life Science Journal*, Vol 6, No 4, 2009.
 9. S. Chatelin, C. Deck, F. Renard, S. Kremer, C. Heinrich, J.-P. Armspach, R. Willinger, "Computation of axonal elongation in head trauma finite element simulation," *Journal of the Mechanical Behavior of Biomedical Materials*, Vol. 4, pp. 1905-1919, 2011.
 10. X. Li, Z. Yin, L. Wei, S. Wan, W. Yu, M. Li. "Symmetry and template guided completion of damaged skulls," *Computers & Graphics*, Vol. 35 (4), pp. 885-893, 2011.
 11. S.M. Badawi, W.A. E. Ahmed, Y.M. Kadah, "Magnetized water and saline as a Contrast agent to Enhance MRI Images", *Life Science Journal*, Vol. 8, Issue 1, 2011.
 12. A. Bartsch, E. Benzel, V. Miele, D. Morr, V. Prakash, "Hybrid III anthropomorphic test device (ATD) response to head impacts and potential implications for athletic headgear testing", *Accident Analysis and Prevention*, Vol. 48, pp. 285-291, 2012.
 13. B.W. Huang, M.Y. Huang, J.-G. Tseng, C.H. Chang, F.-S. Wang, A.D. Lin, Y.C. Tsai, "Dynamic Characteristics of a Hollow Femur," *Life Science Journal*, Vol. 9, No.1, pp. 723-726, 2012.
 14. J.C. Roberts, T.P. Harrigan, E.E. Ward, T.M. Taylor, M.S. Annett, A.C. Merkle, "Human head-neck computational model for assessing blast injury," *Journal of Biomechanics*, Vol. 45, No.16, pp.2899-906, 2012.
 15. C.W. Wei, "An investigation on the dynamic properties of a human brain with impulse", Master Thesis, Graduate Institute of Mechatronics Engineering Cheng Shiu University, 2011.
 16. B.W. Huang, H.K. Kung, K.Y. Chang, P.K. Hsu, J.-G. Tseng, "Human Cranium Dynamic Analysis," *Life Science Journal*, Vol. 6, No.4, pp. 15- 22, 2009.
 17. S. Kleiven, H. Holst, "Consequences of head size following trauma to the human head", *Journal of Biomechanics*, Vol. 35, pp. 153-160, 2002.
 18. H. C. Tzeng, "Modal Testing of Human Heads", Graduate National Yang-Ming Medical College Institute of Biomedical Engineering Master Thesis, 1992.
 19. H.D. Chiu, "Finite Element Analysis of the Dynamic Characteristics of Human Head", Graduate National Yang-Ming Medical College Institute of Biomedical Engineering Master Thesis, 1992.

3/14/2013